This article has been accepted for publication in a future issue of this journal, but has not been fully edited. Content may change prior to final publication. Citation information: DOI 10.1109/TAP.2019.2950817, IEEE Transactions on Antennas and Propagation



# Doubly Curved Reflectarray for Dual-Band Multiple Spot Beam Communication Satellites

Min Zhou, *Member, IEEE,* Stig B. Sørensen, *Member, IEEE,* Yan Brand, and Giovanni Toso, *Senior Member, IEEE*

***Abstract*—The design, manufacturing, and testing of a 0.65-meters doubly curved polarization selective reflectarray for dual-band multiple spot beam communication satellites in Ka-band is presented. The configuration is based on a single-offset reflectarray consisting of rotated split hexagonal-loop dipole elements printed on a single-layer substrate. For RHCP, the reflectarray scans the reflected beam half a beamwidth in one direction, and for LHCP, the reflectarray scans the reflected beam half a beamwidth in the opposite direction. This is achieved in both Tx (17.7-20.2 GHz) and Rx (27.5-29.3 GHz) frequency bands. Using a feeding array with 22 feeds, 41 beams over the Earth can be generated, permitting to cover the entire Earth coverage from a geostationary satellite employing the 4-color frequency/polarization re-use scheme using only two reflectarrays while maintaining single-feed-per-beam operation. The reflectarray has been manufactured and measured, and an excellent agreement between simulated and measured patterns is obtained, thus validating the proposed concept.**

***Index Terms*—Multiple beam antennas, reflectarray, optimization, satellite antenna, circular polarization**

## I. Introduction

MULTIPLE spot beam antennas are becoming more and more popular for telecommunication applications for high-throughput satellites (HTS). Currently, the most mature and reliable antenna architecture is based on four dual-band single-feed-per-beam (SFB) reflectors to cover a multiple beam coverage using the 4-color re-use scheme (see Fig. 1), one reflector for each of the colors for both transmit/receive (Tx/Rx) frequency bands [1], [2]. Despite its maturity and simplicity, this architecture based on four main reflectors exhibits some limitations in terms of reconfigurability (in pattern and power), high mass, and volume. In addition, it requires accurate pointing systems, in order to maintain the four color beams perfectly aligned, and a redundancy scheme because the failure of a single high power feed implies the complete loss of the corresponding beam. In order to remove part of these limitations, several innovative architectures have been proposed in the last years.

Recent developments on feed systems for multiple-feed-per-beam (MFB) reflector antennas have demonstrated that a full multiple spot beam coverage for both Tx/Rx operation can be achieved using only two reflectors. In [3], it is proposed to use dual-band reflectors such that one reflector covers two of the colors in both Tx/Rx and another reflector covers the remaining colors, leading to two dual-band (Tx/Rx) reflectors. Another concept is to use a single reflector to cover all the colors in either Tx or Rx, resulting in one dedicated reflector for Tx and one dedicated reflector for Rx, again using a total of two reflectors [4]–[6]. Based the latter concept, a full multiple beam coverage using only one reflector has also been suggested by combining two single-band MFB feed systems through a frequency selective sub-reflector [7].

Other promising configurations based on active arrays, array organized in overlapped subarrays and discrete active lenses have been recently proposed in order to reduce the number of main apertures and to offer additional flexibility and reconfigurability [8]–[10]. Despite being able to reduce the number of reflectors, all these innovative antenna architectures require advanced beam forming networks and the performance is inferior compared to SFB reflectors with similar aperture sizes. In addition, MFB reflectors are not suitable for non-regular beam lattices with varying beam sizes.

For SFB configurations, the use of three SFB reflectors was proposed in [11]. However, the reduction in the number of reflectors results in degraded performance compared to the traditional four reflector solution. Another concept based on SFB operation is proposed in [12]. Herein, a dual-band polarizing main reflector that converts linear polarization (LP) to circular polarization (CP) is used together with a gridded subreflector to cover half of the beams in both Tx/Rx, leading to a total

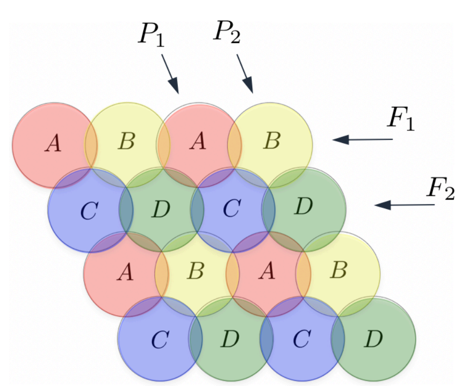


Fig. 1. Beam schematic of the 4-color frequency ($F_1, F_2$) and polarization ($P_1, P_2$) re-use scheme.

Manuscript received xxxx, 2019.

M. Zhou and S.B. Sørensen are with TICRA, Copenhagen, Denmark (e-mail: mz@ticra.com)

Y. Brand is with SYBB Consultants Inc., Montreal, Canada

G. Toso is with the European Space Agency ESA-ESTEC, Noordwijk, The Netherlands (e-mail: giovanni.toso@esa.int)

Color versions of one or more of the figures in this paper are available online at http://ieeexplore.ieee.org.

Digital Object Identifier xxxxxxxx

This article has been accepted for publication in a future issue of this journal, but has not been fully edited. Content may change prior to final publication. Citation information: DOI 10.1109/TAP.2019.2950817, IEEE Transactions on Antennas and Propagation



of two main reflectors to cover the full coverage. The gridded subreflector is needed to separate the two orthogonal linear polarizations at the feed cluster level. As an alternative to the gridded subreflector, one can use a dual-band reflectarray subreflector to separate the two linear polarizations [13]. In a similar manner, the subreflector can also be a dual-band circular polarization selective surface [14]. In this way, the main reflector can be a conventional metallic reflector and does not need to convert the polarization from LP to CP. Common for these concepts is that they rely on the use of dual-reflector systems which increase the complexity of the antenna system.

In [15], a reflectarray concept to reduce the number of apertures, while considering a single-offset antenna system and maintaining SFB operation, is proposed. The idea is to use a parabolic polarization selective reflectarray that can radiate two of the colors in the 4-color re-use scheme. In particular, for one impinging polarization the reflectarray creates a reflected beams tilted in one direction as compared to the specular reflection direction, while for the opposite polarization the reflectarray creates a reflected beams tilted in the opposite direction. It is important to note that a single horn in dual polarization is able to generate two separate beams via the reflectarray. In this way, one reflectarray can generate two of the four colors and another reflectarray can generate the remaining colors, resulting in a total of two apertures to cover the full multiple beam coverage. The concept can be applied for both LP and CP.

In [15], the concept in CP was shown for the Tx-band (20 GHz) using a design consisting of rotated dipoles. In a similar work [16], the idea was demonstrated using a planar reflectarray consisting of two orthogonal sets of three coplanar dipoles. Other work on polarization selective reflectarrays involve the use of polarizers as shown in [17], [18]. However, common for the work in [15]–[18] is that the polarization selectivity is only achieved for the Tx-band only.

In this paper, the polarization selective reflectarray concept is demonstrated for both Tx (19 GHz) and Rx (29 GHz) frequency bands. To this end, a 0.65-meters doubly curved polarization selective reflectarray is designed, manufactured, and measured for the first time. The reflectarray is based on a single-layer design and uses the variable rotation technique (VRT) [19], [20] to control the phase of the reflected field in both Tx and Rx. As array element, the split hexagonal-loop dipole element is used and the reflectarray is designed to radiate half of the beams (two colors) in a global coverage. The manufactured reflectarray is, to the best of the authors knowledge, the first doubly curved reflectarray that has been manufactured. Excellent agreement is obtained between simulations and measurements.

This paper is organized as follows. The reflectarray concept is briefly outlined in Section II. The design of the curved reflectarray is given Section III, this includes the description of the reflectarray configuration, the design specifications, the choice of array elements, the analysis and optimization methods, the RF design, and the evaluation of the antenna performance. The manufacturing of the reflectarray demonstrator is described in Section IV followed by experimental validation in Section V. Conclusions are given in Section VI.

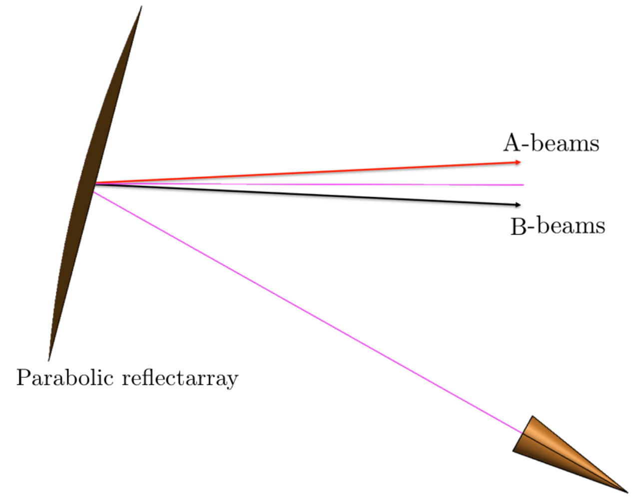


Fig. 2. The concept of the polarization selective reflectarray. A single reflectarray can radiate two of the colors in the 4-color re-use scheme.

## II. Polarization Selective Reflectarray

Reflectarrays can be designed to redirect the reflected beams in a given direction and to shape them according to certain specifications. Their radiation properties can be adjusted with respect to the polarization as well as frequency, and the large number of degrees of freedom in a reflectarray can be utilized to provide attractive solutions otherwise not possible with existing technologies. The proposed reflectarray concept is introduced in [15] and is briefly explained below.

Essentially, a polarization selective reflectarray is needed, i.e., the response of the reflectarray depends on the polarization of the incident field. For a given dual-CP feed, the reflectarray needs to scan the reflected beam half a beamwidth for one polarization and another half beamwidth in the opposite direction for the orthogonal polarization. In this way, one reflectarray can radiate the $A$- and $B$-beams, as shown in Fig. 2, and another reflectarray can radiate the $C$- and $D$-beams, leading to a total of two reflectarrays for the entire coverage. For full Tx/Rx operation, dual-band array elements are necessary.

At Ka-band, CP is used, hence the reflectarrays need to operate in dual-CP for both Tx/Rx. Conventional array elements for CP, e.g., circular/rectangular patches/loops, works in dual-CP, however, the two orthogonal polarizations can not be controlled independently. The challenge lies in the fact that the array elements need to both collimate the beam as well as discriminating the response in dual-CP. To this end, the curvature of the reflectarray can be an additional degree of freedom that can be utilized to achieve polarization selectivity in dual-CP.

Doubly curved reflectarrays were first proposed in [21] and later investigated in [22]–[24] with the goal to improve the bandwidth of shaped beam reflectarrays. For the application at hand, a parabolic surface can be used to collimate the beam such that the array elements only need to discriminate the response in polarization. To this end, the VRT [19] can be applied. Using the VRT, the phase of the reflected field is controlled by the rotation of the array elements. When an array element is illuminated by a CP wave, a rotation of the array

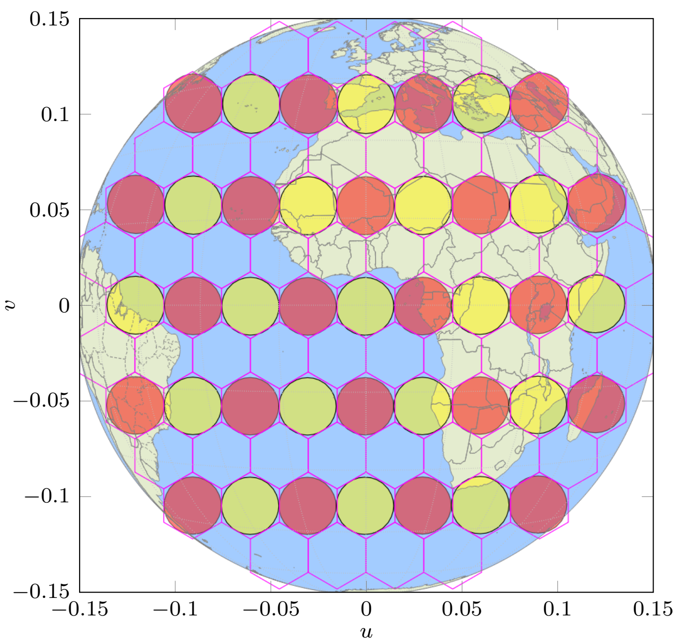


Fig. 3. Beam layout for the reflectarray. The red beams corresponds to RHCP and the yellow beams to LHCP. There are in total 41 beams with a beam spacing of 1.8°.

element by an angle $\psi$ gives the reflected field a phase shift of $\pm 2\psi$ depending on the polarization of the incident field. Using the VRT in conjunction with a parabolic surface, it is possible for a single reflectarray to radiate two of the colors.

Planar reflectarrays can also be applied as demonstrated for the Tx-band in [16]–[18]. However, to achieve dual-band (Tx/Rx) dual-CP operation with polarization selectivity is challenging and is subject to future work. In addition, planar reflectarrays have poor scanning capabilities [25] and the performance deteriorates compared to curved reflectarray for large beam scans which is often required in multiple spot beam applications. Furthermore, with the parabolic surface, only a phase shift of 180° over the surface of the reflectarray is required whereas multiple cycles of 360° may be needed for a planar reflectarray. The many cycles complicate the design and may limit the performance.

## III. Curved Reflectarray Design

### A. Reflectarray Configuration

For the reflectarray, a standard single-offset configuration is considered. The reflectarray surface is a paraboloid surface with a focal length of 1.0 m. The projected aperture diameter is 0.65 m with an aperture center offset of 0.6 m.

As feed, a circular horn designed for a flight mission by MDA is used. It has a diameter of 66 mm and operates in dual-CP at Tx: $18.8 - 19.3$ GHz and Rx: $28.7 - 28.9$ GHz.

### B. Design Specifications

The reflectarray is designed to radiate the two colors in the 4-color re-use scheme that are discriminated in polarization ($P_1$ and $P_2$). The design specifications are listed in Table I and the beam layout is shown in Fig. 3 with $u = \sin(\theta)\cos(\phi)$

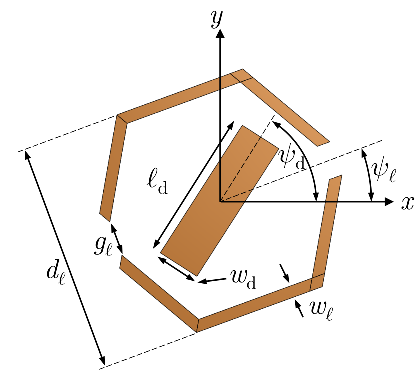


Fig. 4. Split hexagonal-loop dipole element.

and $v = \sin(\theta)\sin(\phi)$. The total number of beams is 41 with a beam spacing of 1.8°. The red and yellow beams in Fig. 3 correspond to right-hand circular polarization (RHCP) and left-hand circular polarization (LHCP), respectively. The peak gain, cross-polarization discrimination (XPD), and carrier-to-interference (C/I) specifications in Table I are based on values that are achieved using traditional reflectors with identical aperture sizes.

Note that the frequency bands listed in Table I are the bands where the horn operates. The bandwidth is quite narrow, 0.5 GHz in Tx and 0.2 GHz in Rx. For some applications a bandwidth of 0.5 GHz in both Tx/Rx is sufficient whereas for other application a bandwidth of 1.25 GHz is needed. As one will see later in Section V, the bandwidth is not a criticality.

### C. Array Element

Many types of array elements that can be used with the VRT have been proposed in the literature, e.g., single dipoles [15], two orthogonal sets of three parallel dipoles [16], concentric split loop elements [20], [26], split loop Malta Cross elements [27], [28], split loop dipole elements [29], or a combination of these. Many of these designs are based on multi-layered configuration.

There are currently no standard manufacturing technologies for the production of doubly curved reflectarrays and a first demonstrator is yet to be manufactured, therefore the manufacturing process is not straightforward. Singly curved reflectarrays have been manufactured and tested before, e.g., in [30], [31]. However, a singly curved surface makes the manufacturing significantly easier. Consequently, to reduce the risk and uncertainties related to the manufacturing process, it was decided to only consider single layer designs.

The array element used in this work is the split hexagonal-loop dipole element shown in Fig. 4. The array elements are printed on a single layer Duroid substrate (RO4835) with a dielectric constant of 3.66, loss tangent of 0.0037, and a thickness of 1.524 mm, and arranged in a square grid with the dimension $5.0 \times 5.0\,\mathrm{mm}^2$. The idea of the element is that the rotation of the outer loop ($\psi_l$) controls the phase in Tx and the rotation of the inner dipole ($\psi_\mathrm{d}$) the phase in Rx. For different combinations of $\psi_l$ and $\psi_\mathrm{d}$, the remaining parameters shall be adjusted to ensure proper CP to CP conversion, i.e., low cross-polarization for a given incidence angle.

This article has been accepted for publication in a future issue of this journal, but has not been fully edited. Content may change prior to final publication. Citation information: DOI 10.1109/TAP.2019.2950817, IEEE Transactions on Antennas and Propagation



TABLE I
DESIGN SPECIFICATIONS

| Frequency band | Polarization | | Beam spacing | Number of beams | Min. Peak Gain | Min. XPD | C/I |
|---|---|---|---|---|---|---|---|
| | $P_1$ (Red) | $P_2$ (Yellow) | | | | | |
| Tx (18.8-19.3 GHz) | RHCP | LHCP | 1.8° | 41 | 38.75 dBi | 22 dB | 15 dB |
| Rx (28.7-28.9 GHz) | RHCP | LHCP | 1.8° | 41 | 38.75 dBi | 22 dB | 15 dB |

In practice, $\psi_l$ and $\psi_{\rm d}$ can not be adjusted independently. At Tx, the phase of the reflected field is indeed controlled by $\psi_l$ and independent of $\psi_{\rm d}$ since the inner dipole is too small to have any effect. However at Rx, there is a strong coupling between the outer loop and the dipole, resulting in a complicated relation between the phase and the rotations $\psi_l$ and $\psi_{\rm d}$. This effect is well-known [20] and solutions to alleviate this often involves the use of multiple layers or FSS backing [28]. In this work, the issue is resolved by means of direct optimization.

### D. Reflectarray Analysis and Optimization

For the design of the reflectarray, the direct optimization technique proposed in [32], [33] is used. Using a direct optimization approach means that all array elements are optimized simultaneously to directly fulfill the pattern specifications. Since the array elements are optimized in a direct manner, meaning the the direct relation between the optimization variables (array elements) and the optimization goals (radiation pattern) is maintained, local mismatches between the desired and actual element performance can be compensated by other elements. Consequently, designs obtained using a direct optimization approach tends to have improved performance compared to those obtained using in-direct optimization approaches [34].

The analysis method used in the direct optimization technique is based on a spectral domain method of moments assuming local periodicity (SDMoM-LP). The optimization algorithm is a gradient-based non-linear minmax algorithm that is well-suited for large-scale optimization problems. It is the same algorithm used in TICRA's commercial software packages [35].

The use of the SDMoM-LP method for planar reflectarrays have been validated against measurements, e.g., in [32], [33], and the method has been extended in [24] to also be applicable for curved reflectarrays. The accuracy of the method has been verified against full-wave simulations, but has not until now been validated against measurements. As will be shown in Section V, the method is exceptionally accurate for the focal length to diameter ratio ($F/D$) considered in this paper. The method has not been tested for small $F/D$ hence the maximum allowed curvature is currently unknown. The reader is referred to [24], [32], [33] for more details on the direct optimization technique.

### E. RF Design

The split hexagonal-loop dipole element has seven individual parameters that can be optimized. Including all of them in the direct optimization would add unnecessary complexity to the optimization problem. From experience, it is a better approach to include the most important parameters in the optimization.

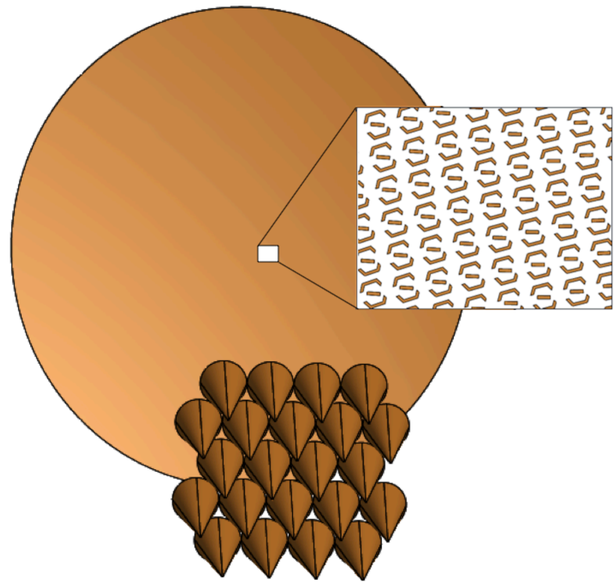

Fig. 5. Reflectarray illuminated by a feedarray consisting of 22 feeds in a hexagonal grid.

As explained in Section III-C, $\psi_\ell$ and $\psi_{\rm d}$ control the phase of the reflected field and the remaining five parameters $(d_\ell, g_\ell, w_\ell, \ell_{\rm d}, w_{\rm d})$ are used to ensure good CP to CP conversion. This means that $\psi_\ell$ and $\psi_{\rm d}$ must be included in the optimization in order to scan the beams. To identify the influence of the remaining parameters, a parametric investigation at the unit-cell level was performed. In this investigation, it was identified that the length of the dipole ($\ell_{\rm d}$) and the gap of the outer loop ($g_\ell$) are the particularly important for the performance. For this reason, in addition to $\psi_\ell$ and $\psi_{\rm d}$, $\ell_{\rm d}$ and $g_\ell$ are also included in the optimization giving a total of four parameters per element. The remaining parameters were kept fixed during the design. The reflectarray consists of 13,508 array elements, yielding a total number of optimization variables of 54,032.

To generate the 41 beams in Fig. 3, 22 feeds are needed and the reflectarray configuration is shown in Fig. 5. Using the direct optimization technique, while taking into account the actual curvature of the surface, the reflectarray is optimized to fulfill the requirements listed in Table I at the center and extreme frequencies of the Tx/Rx band, namely 18.8, 19.05, 19.3, 28.7, 28.8, and 28.9 GHz. For an accurate analysis, spherical wave expansions of the feed pattern are used during the optimization.

Starting the direct optimization with all optimization variables does usually not provide a good design. To ensure

This article has been accepted for publication in a future issue of this journal, but has not been fully edited. Content may change prior to final publication. Citation information: DOI 10.1109/TAP.2019.2950817, IEEE Transactions on Antennas and Propagation



TABLE II
PERFORMANCE COMPARISON, REFLECTARRAY VERSUS REFLECTOR

| | Single Reflectarray | Two Reflectors |
|---|---|---|
| Min. Peak Gain | 38.0 dBi | 38.7 dBi |
| Min. XPD | 22.0 dB | 25.0 dB |
| C/I (> 15 dB) | 71% of coverage | 70% of coverage |
| C/I (> 14 dB) | 100% of coverage | 83% of coverage |
| C/I (> 11 dB) | 100% of coverage | 99% of coverage |

optimal performance, the direct optimization shall be performed in an iterative approach where the number of beams, goal specifications, and optimization variables are gradually increased. As the final step, the optimization is carried out including all beams, goal specifications, and optimization variables, simultaneously.

## *F. Reflectarray Performance*

In Fig. 6, the beams radiated by the optimized reflectarray at the center frequency of the Tx/Rx bands are shown. It is seen that the reflectarray generates 41 beams over the Earth when illuminated by the feedarray. The red and yellow beams represent RHCP and LHCP, respectively. The peak position of the beams are indicated by a cross (+) with the associated peak value. The beam contour level is -4.3 dB below peak.

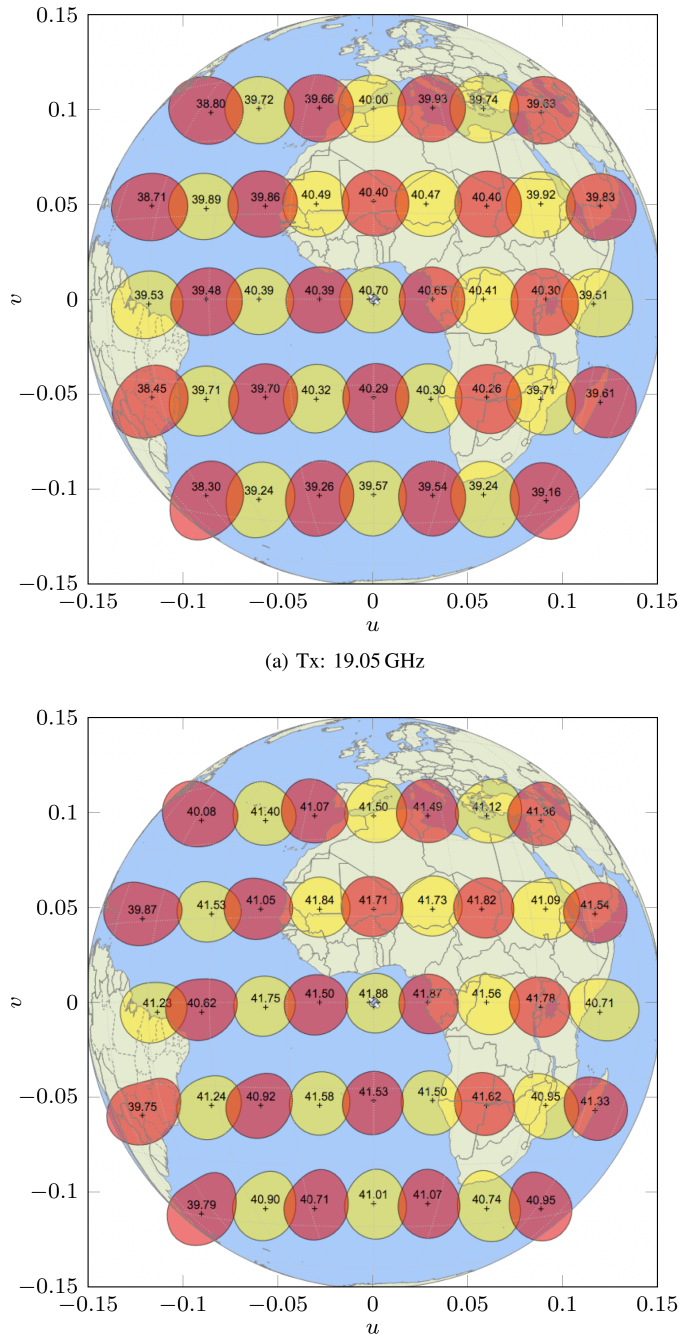


(a) Tx: 19.05 GHz

(b) Rx: 28.8 GHz

Fig. 6. Beams generated by the reflectarray when illuminated by the feedarray. The red and yellow beams represent RHCP and LHCP, respectively. The peak position of the beams are indicated by a cross (+) with associated peak value, and the beam contours show -4.3 dB below peak.

The Tx beams scan quite well with little beam distortion, whereas the distortions for the Rx beams are more visible. Compared to the nominal reflector, the beam shapes of the outer scanned beams are very similar, indicating that the degradation in the gain and beam shape for the scanned beams is mainly due to scan aberrations. The performance in terms of frequency bandwidth will be discussed later.

To evaluate the performance, the gain, XPD, and C/I values of the reflectarray are compared to the ones obtained using two traditional SFB reflectors that generate the same beams as the single reflectarray. The comparison is given in Table II, where the minimum peak gain, minimum XPD, and C/I values are shown. These values are determined by considering all 41 beams in both the Tx and Rx bands for the reflectarray and the two reflectors.

It is seen that the minimum peak gain of the reflectarray is 0.7 dB lower than that of the two reflectors with a value of 38.0 dBi and 38.7 dBi, respectively. For the minimum XPD, the reflectarray is also lower with a value of 22.0 dB compared to 25.0 dB for the reflectors. However, concerning C/I, the reflectarray has a C/I better than 14 dB for the entire coverage, whereas for the reflectors, only 83% of the coverage has a C/I > 14 dB. For the reflectors, the worst case C/I is 10.9 dB. The better C/I performance of the reflectarray is attributed to the fact that the array elements are optimized to improve the C/I performance. It is expected that a similar improvement can be achieved for the reflectors if surface shaping is considered.

It is also observed that the performance of the reflectarray is quite close to the design specifications listed in Table I, as expected. If a different weighting is desired, the performance of the reflectarray can be tailored accordingly by adjusting the optimization goal specifications.

In conclusion, a single SFB reflectarray using only one feedarray is capable of generating the same number of beams as two SFB reflectors using two feedarrays with only a small

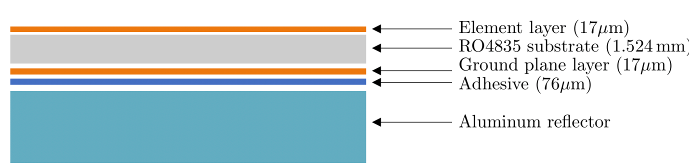


Fig. 7. Reflectarray demonstrator stack-up.

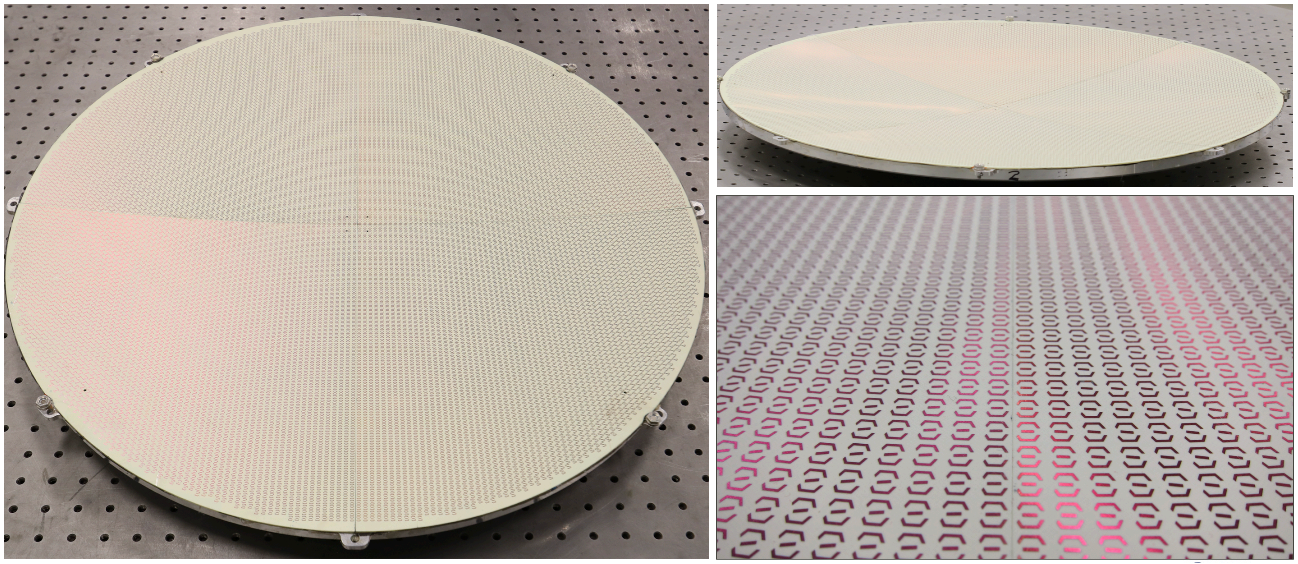

Fig. 8. The manufactured doubly curved reflectarray demonstrator. The boards are cut in quadrants to conform each pie-slice to the doubly-curved surface.

degradation in the gain and XPD performance.

## IV. Manufacturing of the Reflectarray

The purpose of the demonstrator is to demonstrate the proposed reflectarray concept and to confirm the accuracy of the design method. Consequently, to reduce cost, space qualified processes/materials were not considered.

The stack-up used for the reflectarray demonstrator is shown in Fig. 7. For the manufacturing process, the array elements were first printed on planar Duroid boards. An aluminimum reflector was then used as the mold on which the printed boards were conformed and cured. Different curing processes were considered and it was decided to apply a room temperature cured epoxy adhesive using a vacuum forming technique. The boards were cut in four quadrants to help the board to conform to the doubly curved surface. Vacuum was applied during the entire curing phase of the adhesive to keep the board bonded as closely as possible to the surface of the reflector with a constant pressure. For the manufactured antenna, an RMS surface distortion of 0.049 mm was measured.

As the printed board manufacturing process requires a planar surface, it is necessary to distort the printed array element patterns, such that once lay-down to the mold each quadrant conforms as best as possible to the curved mold. The final manufactured reflectarray is shown in Fig. 8. A pin and slot were included on each of the four boards to accurately locate them on the reflector surface.

## V. Experimental Validation

The reflectarray was measured at the compact antenna test range (CATR) at MDA. A feedarray of 22 horns was not available, thus the measurements were carried out using a single horn but positioned at three different locations. The setup for the RF measurements is shown in Fig. 9, where one can see the reflectarray in the CATR at MDA and the three feed configurations. Configuration #1 corresponds to the feed position at the reflector focal point, i.e., the center beams. Configurations #2 and #3 correspond to the outer most scanned beams in the vertical and horizontal planes. In this way, the scan performance of the reflectarray is also experimentally verified. The measurements were carried out for all three configurations in the frequency bands $18.8 - 19.3$ GHz and $28.7 - 28.9$ GHz.

In Fig. 10, the co-polar patterns at the center Tx/Rx frequencies are shown for all three configurations. Measured and simulated patterns are shown in solid and dashed, respectively. The black curves corresponds to LHCP whereas red curves to RHCP. The beam contours show levels at -3, -10, and -20 dB below peak. It is seen that the reflectarray scans the beams for the two orthogonal CP in opposite directions for all three configurations in both Tx and Rx, thus confirming the polarization selectivity of the reflectarray. For the Tx beams, the solid and dashed curves practically coincide, showing an excellent agreement between simulations and measurements. For the Rx beams, some minor discrepancies are present, but the agreement is still very good.

In Fig. 11, the XPD at the center Tx/Rx frequencies are shown for all three configurations. Measured and simulated curves are shown in solid and dashed, respectively. The black curves show LHCP/RHCP and the red RHCP/LHCP. In these figures, the 30 dB XPD curve is shown, meaning that patterns 30 dB below the peak are compared. Some discrepancies between the solid and dashed lines can be observed. However, this is expected as the cross-polar radiation is low and the analysis accuracy and manufacturing tolerances, as well as the measurement errors, come into play. Nonetheless, the general trend and level of the cross-polar radiation is well predicted.

The radiation patterns and agreement between simulations and measurements for the other measured frequencies resemble those shown in Fig. 10 and Fig. 11 and are therefore not shown.

In Section III-A, it was stated that the horn used to illu-

This article has been accepted for publication in a future issue of this journal, but has not been fully edited. Content may change prior to final publication. Citation information: DOI 10.1109/TAP.2019.2950817, IEEE Transactions on Antennas and Propagation



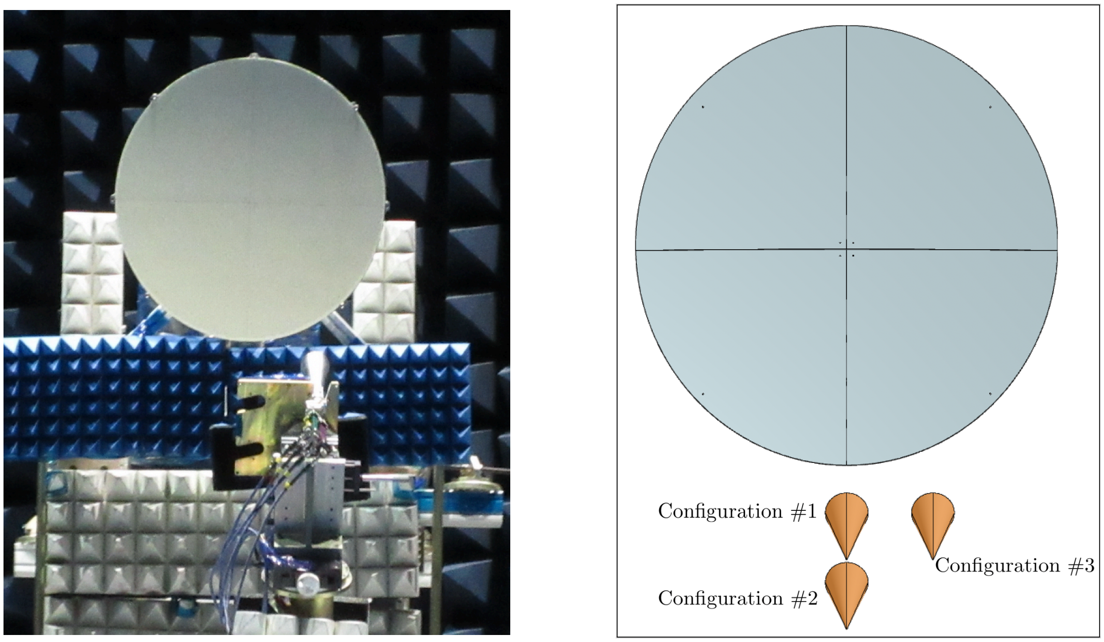


(a) (b)

Fig. 9. The setup for the RF measurements, (a) the reflectarray in the CATR at MDA with the feed in Configuration #3, (b) the three feed configurations that were measured.

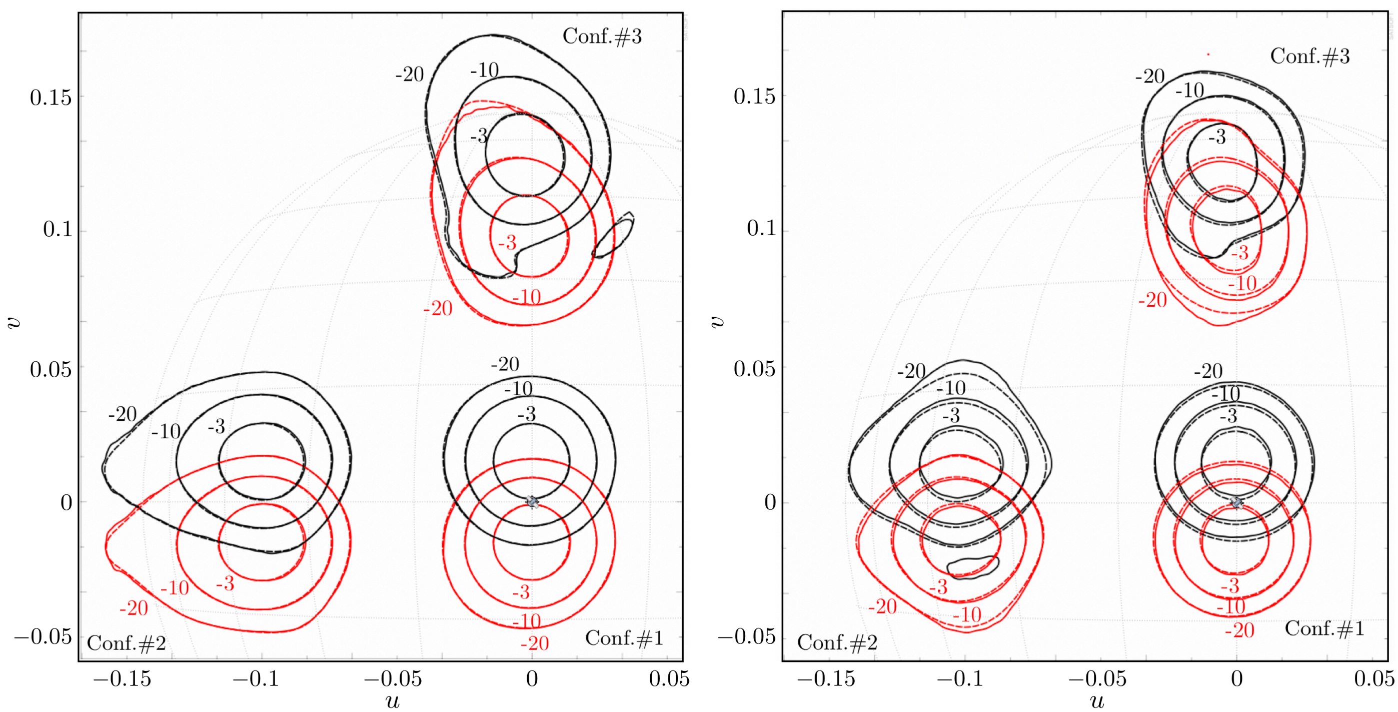


(a) Tx: 19.05 GHz (b) Rx: 28.8 GHz

Fig. 10. Measured (solid) and simulated (dashed) co-polar radiation patterns at the center frequencies of the Tx/Rx band. All three measured configurations are shown. Black and red curves corresponds to LHCP and RHCP, respectively. The beam contours show -3, -10, and -20 dB below peak for each individual beam.

minate the reflectarray operates between 18.8 – 19.3 GHz and 28.7 – 28.9 GHz, which is the reason why the reflectarray was optimized within these bands. After the initial measurements, it was identified that the horn actually could operate over a significnatly wider bands, namely 17.7 – 20.2 GHz and 27.5 – 29.3 GHz. Therefore, a second set of wide band measurements were conducted. In a real HTS mission, only 1.25 GHz bandwidth in both Tx/Rx would be required for this reflectarray. Nonetheless, the entire 2.5 GHz and 1.8 GHz Tx/Rx bands were measured. For this measurement, only Configuration #1 was considered.

In Fig. 12, the measured (solid) and simulated (dashed)

This article has been accepted for publication in a future issue of this journal, but has not been fully edited. Content may change prior to final publication. Citation information: DOI 10.1109/TAP.2019.2950817, IEEE Transactions on Antennas and Propagation



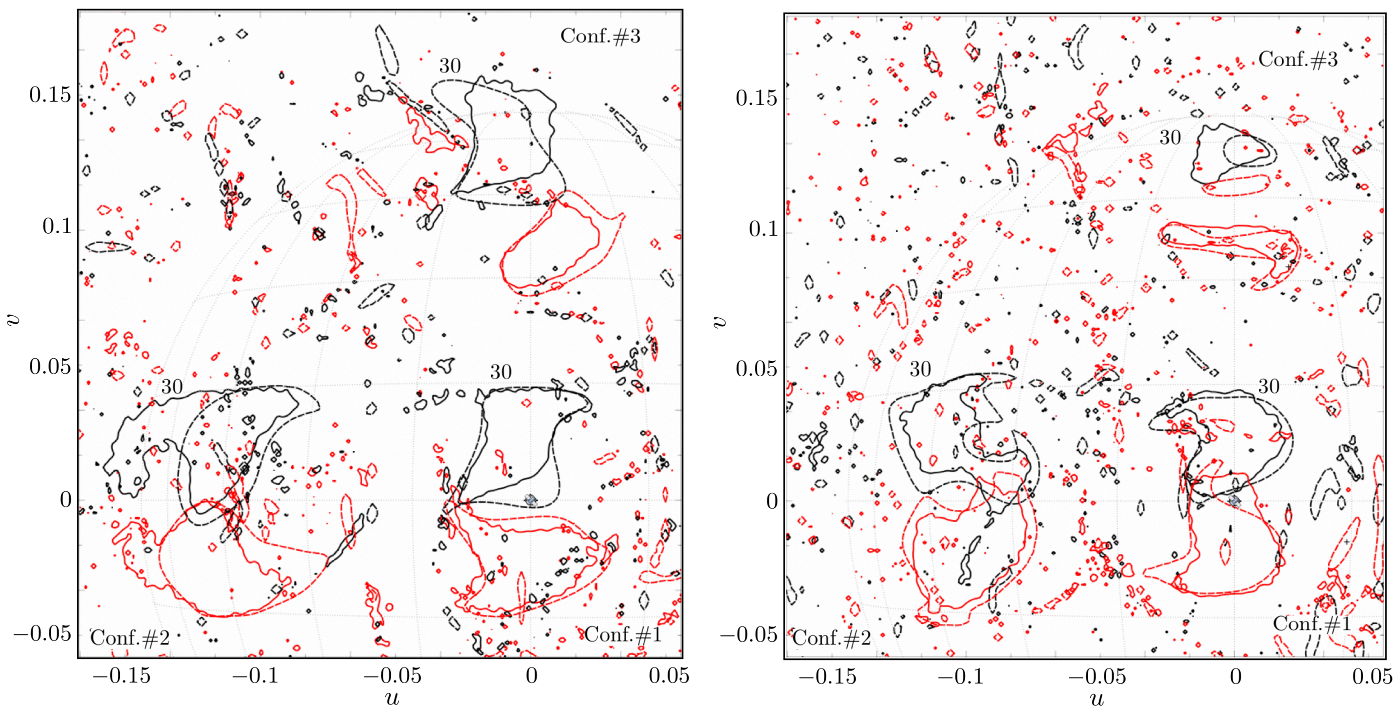


(a) Tx: 19.05 GHz

(b) Rx: 28.8 GHz

Fig. 11. Measured (solid) and simulated (dashed) XPD curves at the center frequencies of the Tx/Rx band. All three measured configurations are shown. Black and red curves corresponds to LHCP/RHCP and RHCP/LHCP, respectively. The beam contours show the 30 dB curve.

co-polar patterns at the extreme frequencies of the Tx/Rx bands are shown. Similar to before, black and red correspond to LHCP and RHCP, respectively. It is observed that the reflectarray still separates the beams in opposite directions for LHCP and RHCP, indicating that the concept is still valid, even though the bandwidth considered in Tx and Rx is 2.5 GHz and 1.8 GHz, respectively, and that the reflectarray is not optimized in these wide band frequency ranges. Excellent agreement is obtained between simulations and measurements.

In Fig. 13, the average of the peak gain of the LHCP and RHCP beams for Configuration #1 is shown as function of frequency. The simulated gain values agree with the measurements within measurement uncertainty in both Tx and Rx. In terms of losses, the predicted and measured (averaged) loss in Tx is 0.1 dB and 0.2 dB, respectively, and in Rx 0.2 dB and 0.4 dB, respectively. The gain variation is less than 2 dB in the entire Tx/Rx bands. To compare the variation of that of the nominal reflector, the average peak directivity of the reflector is also shown in Fig. 13. It is seen that the gain variation of the reflectarray follows closely that of the nominal reflector, indicating similar bandwidth as the reflector.

The XPD and C/I performance of the reflectarray deteriorates outside the design frequencies, which is expected. But since the co-polar gain follows that of the reflector and the beams are still discriminated in dual-CP in both Tx/Rx, it is expected that a significant portion of the performance can be recuperated after proper re-optimization. This is subject to future work.

The next step in the development of the proposed concept would be to proceed with a full qualification campaign, including thermal cycling, vibration tests, etc.

## VI. Conclusions

In this paper, the design, manufacturing, and testing of a doubly curved polarization selective reflectarray for dual-band multiple beam application in Ka-band is presented. The proposed reflectarray concept can cover a full multiple beam coverage using the 4-color frequency/polarization re-use scheme using only two offset single-feed-per-beam reflectarrays in both Tx and Rx. The concept relies on the use of a parabolic reflectarray in conjunction with the variable rotation technique.

To demonstrate the concept, a doubly curved reflectarray that covers half of the beams needed in the full coverage has been designed and manufactured. It is to the knowledge of the authors the first time that a doubly curved reflectarray has been successfully manufactured. Excellent agreements between simulations and measurements are obtained, demonstrating the high accuracy of the simulation methods and the manufacturing process. The experimental results also demonstrate the concept in wide frequency bands between $17.7 - 20.2$ GHz and $27.5 - 29.3$ GHz, indicating that it can cover realistic mission requirements. These results show that curved reflectarrays are viable candidates to be used on future multiple spot beam communication satellites.

## Acknowledgment

The authors would like to thank Jordan Bellemore and Simon Maltais for their assistance throughout the development. They would also like to thank Geraud De Belleville for performing the RF measurements at the CATR at MDA.

This article has been accepted for publication in a future issue of this journal, but has not been fully edited. Content may change prior to final publication. Citation information: DOI 10.1109/TAP.2019.2950817, IEEE Transactions on Antennas and Propagation



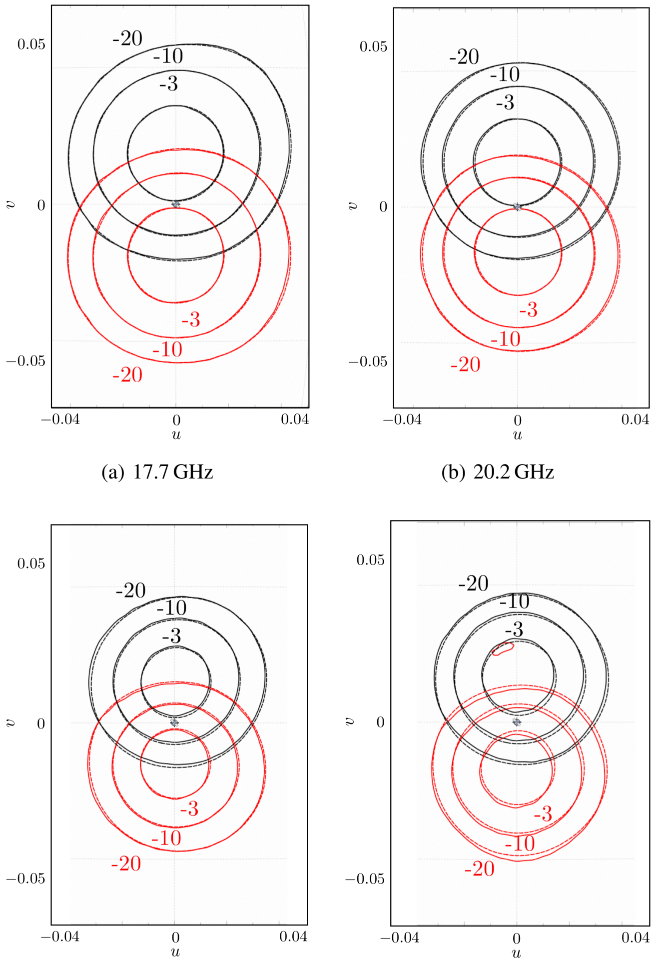


(a) 17.7 GHz (b) 20.2 GHz

(c) 27.5 GHz (d) 29.3 GHz

Fig. 12. Measured (solid) and simulated (dashed) co-polar radiation patterns at the extreme frequencies of the Tx/Rx band for Conf.#1. Black and red curves correspond to LHCP and RHCP, respectively. The beam contours show -3, -10, and -20 dB below peak.

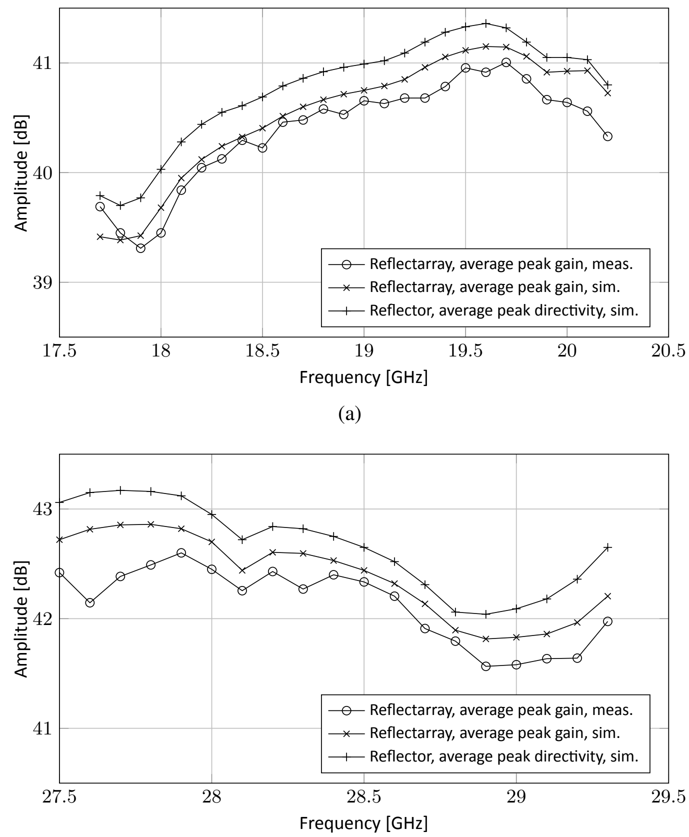


(a)

(b)

Fig. 13. Measured and simulated average peak gain for Conf.#1 for (a) the Tx band and (b) the Rx band. To compare the variation of that of the nominal reflector, the average peak directivity of the reflector is also shown.

## References


[1] E. Amyotte, Y. Demers, L. Hildebrand, M. Forest, S. Riendeau, S. Sierra-Garcia, and J. Uher, "Recent developments in Ka-band satellite antennas for broadband communications," in *Proc. EuCAP*, 2010.

[2] S. K. Rao, "Parametric design and analysis of multiple-beam reflector antennas for satellite communications," *IEEE Antennas Propag. Mag.*, vol. 45, no. 4, pp. 25–34, 2003.

[3] J. C. Lafond, E. Vourch, F. Delepaux, P. Lepeltier, P. Bosshard, F. Dubos, C. Feat, C. Labourdette, G. Navarre, and J. M. Bassaler, "Thales Alenia Space multiple beam antennas for telecommunication satellites," in *Proc. EuCAP*, 2014.

[4] J. M. Montero, A. M. Ocampo, and N. J. G. Fonseca, "C-band multiple beam antennas for communication satellites," *IEEE Trans. Antennas Propag.*, vol. 63, no. 4, pp. 1263–1275, 2015.

[5] M. Schneider, C. Hartwanger, E. Sommer, and H. Wolf, "The multiple spot beam antenna project "Medusa"," in *Proc. EuCAP*, 2009.

[6] C. Leclerc, M. Romier, H. Aubert, and A. Annabi, "Ka-band multiple feed per beam focal array using interleaved couplers," *IEEE Trans. Microwave Theory Tech.*, vol. 62, no. 6, pp. 1322–1329, 2014.

[7] N. J. G. Fonseca, "Dual-band (Tx/Rx) multiple-beam reflector antenna using a frequency selective sub-reflector for Ka-band applications," in *Proc. EuCAP*, Lisbon, Portugal, 2015.

[8] P. Angeletti, G. Toso, and G. Ruggerini, "Array antennas with jointly optimized elements positions and dimensions part ii: Planar circular arrays," *IEEE Trans. Antennas Propag.*, vol. 62, no. 4, pp. 1627–1639, 2014.

[9] D. Petrolati, P. Angeletti, and G. Toso, "A lossless beam-forming network for linear arrays based on overlapped sub-arrays," *IEEE Trans. Antennas Propag.*, vol. 62, no. 4, pp. 1769–1778, 2014.

[10] G. Toso, P. Angeletti, G. Ruggerini, and G. Bellaveglia, "Active aperiodic lens for multibeam satellite coverages," *European Patent 2221919*, August 2010.

[11] E. Amyotte, Y. Demers, V. Dupessey, M. Forest, L. Hildebrand, A. Liang, M. Riel, and S. Sierra-Garcia, "A summary of recent developments in satellite antennas at MDA," in *Proc. EuCAP*, 2011.

[12] N. J. G. Fonseca and C. Mangenot, "High-performance electrically thin dual-band polarizing reflective surface for broadband satellite applications," *IEEE Trans. Antennas Propag.*, vol. 64, no. 2, pp. 640–649, 2016.

[13] D. M. de Rioja, E. M. de Rioja, J. A. Encinar, A. Pino, Y. Rodriguez-Vaqueiro, B. Gonzalez-Valdes, O. Rubinos, and M. Arias, "Single and dual reflectarray configurations for multibeam satellite antennas in Ka-band," in *Proc. EuCAP*, 2019.

[14] J. Sanz-Fernandez, E. Saenz, P. de Maagt, and C. Mangenot, "Circular polarization selective surface for dual-optics CP offset reflector antennas in Ku-band," in *Proc. EuCAP*, Prague, Czech Republic, 2012.

[15] M. Zhou and S. B. Sørensen, "Multi-spot beam reflectarrays for satellite telecommunications applications in Ka-band," in *Proc. EuCAP*, Davos, Switzerland, 2016.

[16] R. Florencio, J. A. Encinar, R. R. Boix, M. Barba, and G. Toso, "Flat reflectarray that generates adjacent beams by discriminating in dual circular polarization," *To be published in IEEE Trans. Antennas Propag.*, 2019.

[17] M.-A. Joyal, R. E. Hani, M. Riel, Y. Demers, and J.-J. Laurin, "A reflectarray-based dual-surface reflector working in circular polarization," *IEEE Trans. Antennas Propag.*, vol. 63, no. 4, pp. 1306–1313, 2015.

[18] C. Geaney, M. Hosseini, and S. Hum, "Reflectarray antennas for independent dual linear and circular polarization control," *To be published in IEEE Trans. Antennas Propag.*, 2019.

[19] J. Huang and R. J. Pogorzelski, "A Ka-band microstrip reflectarray

with elements having variable rotation angles," *IEEE Trans. Antennas Propag.*, vol. 46, no. 5, pp. 650–656, 1998.

[20] T. Smith, U. Gothelf, O. S. Kim, and O. Breinbjerg, "Design, manufacturing, and testing of a 20/30-GHz dual-band circularly polarized reflectarray antenna," *IEEE Antennas Wireless Propag. Lett.*, vol. 12, pp. 1480–1483, 2013.

[21] M. E. Cooley, T. J. Chwalek, and P. Ramanujam, "Method for improving pattern bandwidth of shaped reflectarrays," *US Patent 6,031,506*, February 2000.

[22] J. A. Encinar, M. Arrebola, and G. Toso, "A parabolic reflectarray for a bandwidth improved contoured beam coverage," in *Proc. EuCAP*, Edinburgh, UK, 2007.

[23] C. Tienda, M. Arrebola, J. A. Encinar, and G. Toso, "Analysis of parabolic reflectarray in dual-reflector configuration," in *Proc. EuCAP*, Barcelona, Spain, 2010.

[24] M. Zhou, S. B. Sørensen, O. Borries, and E. Jørgensen, "Analysis and optimization of a curved transmit-receive contoured beam reflectarray," in *Proc. EuCAP*, Lisbon, Portugal, 2015.

[25] S. R. Rengarajan, "Scanning and defocusing characteristics of microstrip reflectarrays," *IEEE Antennas Wireless Propag. Lett.*, vol. 9, pp. 163–166, 2010.

[26] T. Smith, U. Gothelf, O. S. Kim, and O. Breinberg, "An FSS-backed 20/30 GHz circularly polarized reflectarray for a shared aperture L- and Ka-band satellite communication antenna," *IEEE Trans. Antennas Propag.*, vol. 62, no. 2, pp. 661–668, 2014.

[27] R. Deng, Y. Mao, S. Xu, and F. Yang, "A single-layer dual-band circularly polarized reflectarray with high aperture efficiency," *IEEE Trans. Antennas Propag.*, vol. 63, no. 7, pp. 3317–3320, 2015.

[28] R. Deng, F. Yang, S. Xu, and M. Li, "An FSS-backed 20/30-GHz dual-band circularly polarized reflectarray with suppressed mutual coupling and enhanced performance," *IEEE Trans. Antennas Propag.*, vol. 65, no. 2, pp. 926–931, 2017.

[29] C. Han, C. Rodenbeck, J. Huang, and K. Chang, "A C/Ka dual frequency dual layer circularly polarized reflectarray antenna with microstrip ring elements," *IEEE Trans. Antennas Propag.*, vol. 52, no. 11, pp. 2871–2876, 2004.

[30] M. Beccaria, P. Pirinoli, G. Dassano, and M. Orefice, "Design and experimental validation of convex conformal reflectarray antennas," *Electron. Lett.*, vol. 52, no. 18, pp. 1511–1512, 2016.

[31] M. Cooley, "Phased array fed reflector (PAFR) antenna architectures for space-based sensor," in *Proc. IEEE Aerospace Conference*, 2015.

[32] M. Zhou, S. B. Sørensen, O. S. Kim, E. Jørgensen, P. Meincke, and O. Breinbjerg, "Direct optimization of printed reflectarrays for contoured beam satellite antenna applications," *IEEE Trans. Antennas Propag.*, vol. 61, no. 4, pp. 1995–2004, 2013.

[33] M. Zhou, S. B. Sørensen, O. S. Kim, E. Jørgensen, P. Meincke, O. Breinbjerg, and G. Toso, "The generalized direct optimization technique for printed reflectarrays," *IEEE Trans. Antennas Propag.*, vol. 62, no. 4, pp. 1690–1700, 2014.

[34] M. Zhou, O. Borries, and E. Jørgensen, "Design and optimization of a single-layer planar transmit-receive contoured beam reflectarray with enhanced performance," *IEEE Trans. Antennas Propag.*, vol. 63, no. 3, pp. 1247–1254, 2015.

[35] TICRA, Denmark, *www.ticra.com*.

**Min Zhou** (S'12–M'13) was born in 1984 in Beijing, China. He received the M.Sc. degree in electrical engineering from the Technical University of Denmark (DTU), Lyngby, Denmark, in 2009, and the Ph.D. degree in 2013 at the same university.

Since 2009, he has been with the Danish company TICRA, Copenhagen, Denmark, where he has mainly worked on the analysis and optimization of printed reflectarrays. His research interest include computational electromagnetics, antenna theory, and analysis and design techniques for quasi-periodic surfaces such as reflectarrays and frequency selective surfaces.

M. Zhou received DTU's Young Researcher Award for his Ph.D. work on reflectarrays in 2013. He was also the recipient of the Best Innovative Paper Award at the 36th and 40th ESA Antenna Workshop in 2015 and 2019, respectively.

**Stig B. Sørensen** was born in Denmark, in 1958. He received the M.Sc. degree and the Industrial Research Education degree from the Technical University of Denmark (DTU), Lyngby, in 1982 and 1985, respectively.

Since 1983, he has been with TICRA, Copenhagen, Denmark, where he has been involved in the development of most of the TICRA software packages and the associated numerical electromagnetic methods. His research interest include computational electromagnetics, quasi optical systems, and analysis and synthesis of shaped reflector antennas and printed reflectarrays.

**Yan Brand** was born in Geneva, Switzerland, on May 11, 1965. His training includes certified electromechanics in 1985. He received the B.S.E.E.degree (with honors) from the Geneva Technical School, Geneva, in 1989 and the M.S.E.E. degree in telecommunications and the Ph.D. degree in applied electromagnetics from the Swiss Federal Institute of Technology, Lausanne, Switzerland, in 1993 and 1996, respectively.

From 1996 to 1997, he participated in the development of a 650 GHz quasi-optic feed for radiometric applications as a Postdoctoral Researcher. From 1997 to 2001, he was with the Swiss Center for Electronics and Micro-Technologies as a Project Manager and Senior RF Engineer involved in the conception, realization, and industrialization of customized application specific RF modules and transceivers as well as air to ground RF propagation studies. From 2001 to 2008, he was with MDA Space Missions (formerly EMS-Technologies), Montreal, PQ, Canada, as a Senior Antenna Engineer, principally involved in research and development for space and avionic antenna systems. From 2008 to 2014 he was working as an Antenna Engineer in the Payload Procurement Group at Eutelsat S.A, and was involved in all aspects of spacecraft antennas, from Mission definition to In-Orbit measurements. From 2014 to 2019 he worked at MDA Corporations, Montreal, Canada, as Senior Product Development Manager, involved in new antenna developments and front-line of the Business. He is currently working as independent consultant at SYBB Consultants Inc., Montreal, Canada.

**Giovanni Toso** (S'93–M'00–SM'07) ) received the Laurea Degree (cum laude), the Ph.D. and the Post Doctoral Fellowship from the University of Florence, Italy, in 1992, 1995 and 1999. In 1996 he was visiting scientist at the Laboratoire d'Optique Electromagnétique, Marseille (France). In 1999 he was a visiting scientist at the University of California (UCLA) in Los Angeles, he received a scholarship from Alenia Spazio (Rome, Italy) and he has been appointed researcher in a Radio Astronomy Observatory of the Italian National Council of Researches (CNR). Since 2000 he is with the Antenna and Submillimeter Waves Section of the European Space Agency, ESA ESTEC, Noordwijk, The Netherlands. He has been initiating and contributing to several R&D activities on satellite antennas based on arrays, reflectarrays, lenses and reflectors.

G. Toso has been coauthoring the best paper at the 30th ESA Antenna Workshop and the most innovative paper at the 30th and 36th ESA Antenna Workshops. In 2009 he has been coeditor of the Special Issue on Active Antennas for Satellite Applications in the International Journal of Antennas and Propagation. In 2014 he has been guest editor, together with Dr. R. Mailloux, of the Special Issue on "Innovative Phased array antennas based on non-regular lattices and overlapped subarrays" published in the IEEE Transactions on Antennas and Propagation and, for the same society, has been an Associate Editor (2013-2016). Since 2010, together with Dr. P. Angeletti, he has been instructing short courses on Multibeam Antennas and Beamforming Networks during international conferences (IEEE APS, IEEE IMS, IEEE IWCS, EUCAP, EuMW) that have been attended by more than 600 participants. In 2018, G. Toso received with Prof. A. Skrivervik the Best Teacher Award of the European School of Antennas (ESoA) out of 101 teachers.